Molecular studies of the initiation and termination steps of the anionic polymerization of P=C bonds

Bronwyn H. Gillon, Kevin J.T. Noonan, Bastian Feldscher, Jennifer M. Wissenz, Zhi Ming Kam, Tom Hsieh, Justin J. Kingsley, Joshua I. Bates, and Derek P. Gates

Abstract: The initiation and termination steps of the anionic polymerization of P=C bonds have been modeled. The initiation step was investigated through the stoichiometric reaction of $MesP{=}CPh_2$ (**1**) with RLi (R = Me or *n*-Bu). In each case, the addition was highly regioselective with the formal attack of R^- at phosphorus to give the carbanion $Li[Mes(R)P–CPh_2]$ (**3a**, R = Me; **3b**, R = *n*-Bu). To simulate the termination step in the anionic polymerization of **1**, carbanions **3a** and **3b** were quenched in situ with various electrophiles. Through these reactions, several new tertiary phosphines have been prepared, namely, $Mes(Me)P–CPh_2H$ (**4a**), $Mes(n\text{-}Bu)P\text{-}CPh_2H$ (**4b**), $Mes(Me)P–CPh_2Me$ (**6a**), $Mes(Me)P–CPh_2–P(NEt_2)_2$ (**7a**), $Mes(Me)P–CPh_2–SiMe_2H$ (**8a**), and $Mes(Me)P–CPh_2–SiMe_3$ (**9a**). In addition, compounds **4a**, **7a**, **8a**, and **9a** were characterized by X-ray crystallography. Most of the metrical parameters are typical of tertiary phosphines; however, the $P–CPh_2H$ bonds were elongated in all cases reflecting the considerable steric bulk surrounding this bond. Unexpectedly, an unusually large $^{31}P–^{31}P$ coupling constant ($^2J_{PP} > 200$ Hz) was observed for **7a** both in solution and the solid state. This observation may be rationalized by a through space P···P interaction. This rationale is further supported by the short P···P distance [P(1)—P(2) = 2.966(1) Å; cf. $\Sigma\ r_{vdw}$ = 3.7 Å] and a small P–C–P bond angle for **7a** [P(1)–C(11)–P(1) = 99.17(9)°].

Key words: phosphaalkenes, phosphorus polymers, phosphines, anionic polymerization.

Résumé : On a développé un modèle pour les étapes d'initiation et de terminaison de la polymérisation anionique des liaisons P=C. On a étudié l'étape d'initiation par le biais de la réaction stoechiométrique du $MesP{=}CPh_2$ (**1**) avec du RLi (R = Me ou Bu). Dans chacun des cas, l'addition est très régiosélective avec une attaque formelle du R^- sur le phosphore pour conduire à la formation du carbanion $Li[Mes(R)P–CPh_2]$ (**3a**, R = Me; **3b**, R = Bu). Dans le but de simuler l'étape de terminaison de la polymérisation du composé **1**, les carbanions **3a** et **3b** ont été piégés in situ avec divers électrophiles. Par le biais de ces réactions, on a obtenu plusieurs nouvelles phosphines tertiaires, soit: $Mes(Me)P–CPh_2H$ (**4a**); $Mes(Bu)P–CPh_2H$ (**4b**); $Mes(Me)P–CPh_2Me$ (**6a**); $Mes(Me)P–CPh_2–P(NEt_2)$ (**7a**); $Mes(Me)P–CPh_2–SiMe_2H$ (**8a**) et $Mes(Me)P–CPh_2–SiMe_3$ (**9a**). De plus, on a caractérisé les composés **4a**, **7a**, **8a** et **9a** par diffraction des rayons X. La plupart des paramètres métriques sont typiques des phosphines tertiaires; toutefois, dans tous les cas, les liaisons $P–CPh_2H$ sont allongées et cette caractéristique reflète l'encombrement stérique important aux abords de cette liaison. D'une façon inattendue, on a observé une constante de couplage $^{31}P–^{31}P$ exceptionnellement élevée ($^2J_{PP} > 200$ Hz) avec le composé **7a**, tant à l'état solide qu'en solution. On peut rationaliser cette observation à l'aide d'une interaction P···P à travers l'espace. Ce raisonnement est supporté par la courte distance P···P [P(1)—P(2) = 2,966(1) Å; cf. $\Sigma\ r_{vdw}$ = 3,7 Å] et un faible angle P–C–P pour le composé **7a** [P(1)–C(11)–P(1) = 99,17(9)°].

Mots-clés : phosphaalcènes, polymères du phosphore, phosphines, polymérisation anionique.

[Traduit par la Rédaction]

Introduction

Phosphaalkenes, compounds with genuine (2p–3p) π bonds, are an intriguing class of low-coordinate phosphorus species. Although the first stable derivatives were reported in the late 1970s, interest in phosphaalkenes continues to grow because of their parallelism to the chemistry of C=C bonds and their potential applications (1–3). For example, compounds with P=C bonds are being explored as ligands in transition-metal-catalyzed reactions (4–7) and in polymer science (8–13).

Recently, we reported the polymerization of phosphaalkene **1** to afford poly(methylenephosphine) **2**, a new functional phosphine polymer with alternating phosphorus and carbon atoms in the main chain (see Scheme 1) (12). Our initial studies suggested that the polymerization of **1** required high temperatures (>150 °C), long reaction times, and high concentrations, even in the presence of radical or anionic initiators. We subsequently showed that short-chain oligomers could be obtained when **1** is treated with anionic

Received 23 July 2007. Accepted 12 September 2007. Published on the NRC Research Press Web site at canjchem.nrc.ca on 22 November 2007.

B.H. Gillon, K.J.T. Noonan, B. Feldscher, J.M. Wissenz, Z.M. Kam, T. Hsieh, J.J. Kingsley, J.I. Bates, and D.P. Gates.[1] Department of Chemistry, University of British Columbia, 2036 Main Mall, Vancouver, BC V6T 1Z1, Canada.

[1] Corresponding author (e-mail: dgates@chem.ubc.ca).

doi:10.1139/V07-121

Scheme 1.

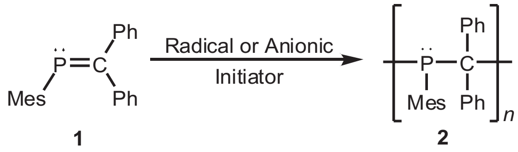

initiators (i.e., MeLi) in THF solution at ambient temperature (14). This solution oligomerization has now been extended to the living anionic polymerization of monomer **1** to afford homopolymer **2** and block copolymers with controllable architectures (11). To further develop the living anionic polymerization of P=C bonds and to prepare end-functionalized polymers, it is necessary to fully understand the mechanism of anionic chain growth for **1**.

To our knowledge, there is little previous work on the reaction of P=C bonds with typical anionic initiators. Of particular relevance to our studies is the synthesis of phosphine oxide **5a** from phosphaalkene **1** (15) (see Scheme 2). Specifically, treating **1** with MeLi followed by MeOH and air oxidation afforded **5a**. Both the carbanion (**3a**) and the phosphine (**4a**) were the proposed intermediates in this reaction. In a separate study, the addition of MeLi to $\mathrm{RP{=}C(SiMe_3)_2}$ (R = Mes, *t*-Bu) afforded $\mathrm{Li[MeRPC(SiMe_3)_2]}$, which was characterized spectroscopically (16–18). In several other studies, the addition of alkyllithium reagents across the P=C bond in phosphinines and triphosphafulvenes similarly afforded only the P-alkyl products (19). These regioselective additions are consistent with the predicted polarity of the P=C bond, based on the electronegativities of phosphorus (δ+) and carbon (δ–). Interestingly, alkyllithium reagents can also react with phosphaalkenes with preservation of the P=C bond (20).

In this paper, we disclose our molecular-model studies of the initiation and termination steps of the anionic polymerization of **1**. Two initiators were chosen for the present studies: MeLi and *n*-BuLi. Although *n*-BuLi is a better initiator for the anionic polymerization of **1** (11, 12), MeLi is optimal in molecular-model studies, since the small Me substituent is more likely to afford crystalline products. The new compounds obtained may be utilized as molecular models for the development of the coordination chemistry of polymer **2**. Moreover, the development of methods to end-functionalize poly(methylenephosphine)s will afford telechelic polymers, which may function as precursors to novel block copolymers.

Results and discussion

The phosphaalkene **1** was prepared according to literature methods (21, 22). A pale-yellow solution of **1** in THF was treated with a slight excess of alkyllithium at low temperatures, resulting in an immediate color change to deep red. Analysis of the reaction mixture using $^{31}\mathrm{P}\{^{1}\mathrm{H}\}$ NMR spectroscopy confirmed the complete conversion of **1** to the carbanion **3a** ($\delta = -44.3$) or to **3b** ($\delta = -31.1$). These intermediates are believed to be related to the active species in the anionic polymerization of **1**.

Carbanion **3a** was quenched by addition of water or methanol to afford model compound **4a** ($\delta_{^{31}\mathrm{P}} = -24.0$). Additionally, $^{13}\mathrm{C}\{^{1}\mathrm{H}\}$, $^{1}\mathrm{H}$ NMR spectroscopy, and low resolution EI-MS ($\mathrm{M^+}$, $m/z = 332$) were consistent with the proposed structure. The $^{1}\mathrm{H}$ NMR spectrum of **4a** shows a notably downfield doublet resonance at $\delta = 4.87$ ($^{2}J_{\mathrm{HP}} = 5$ Hz), which is assigned to the benzylic proton. Importantly, a doublet resonance is observed in the alkyl region ($\delta = 1.31$, $^{2}J_{\mathrm{HP}} = 6$ Hz), which is attributed to the $\mathrm{P{-}CH_3}$ protons. Clearly, addition of the methyl anion occurs regioselectively at the phosphorus atom of the P=C bond. Also found in the alkyl region are sharp singlets at 2.52 and 2.21 ppm that are assigned to the ortho- and para-methyl protons of the mesityl group, respectively.

Clear, colorless crystals suitable for X-ray diffraction were obtained from the slow evaporation of a concentrated solution of **4a** in hexanes. The molecular structure and the crystallographic data appear in Fig. 1, Table 1, and the Supplementary data.[2] The molecular structure provides insight into the steric nature of the substituents around the P atom. Importantly, the cone angle of the model compound **4a** was estimated to be roughly 140°, which is comparable to that of triphenylphosphine (145°) (23).[3] The P—C bond lengths (Å) fall into the typical range for P—C single bonds [P(1)—C(1) = 1.852(1), P(1)—C(10) = 1.840(2), P(1)—C(11) = 1.882(1)] (24). Presumably, steric repulsion is responsible for the slight elongation of P(1)—C(11). For comparison, related P—C bonds where the carbon atom has two aryl substituents (i.e., $\mathrm{RArP{-}CHPh_2}$) are ~1.90 Å in length (25, 26).

Using *n*-BuLi as the initiator for **1**, the related compound **4b**, was prepared by terminating carbanion **3b** with water. Again, the reaction was quantitative as suggested by $^{31}\mathrm{P}\{^{1}\mathrm{H}\}$ NMR spectroscopy ($\delta = -12.4$). Upon workup, analytically pure **4b** was isolated in good yield (85%) as a yellow oil. Akin to the Me-initiated **4a**, the $^{1}\mathrm{H}$ NMR spectrum of *n*-Bu-initiated **4b** showed a characteristic doublet resonance at 4.91 ppm ($^{2}J_{\mathrm{HP}} = 5$ Hz), which is assigned to the benzylic proton. A sharp singlet at 2.20 ppm is assigned to the para-methyl mesityl protons. In contrast to the sharp signals observed for **4a**, the ortho-methyl mesityl protons in **4b** exhibit a broad signal centred at 2.56 ppm. The broadening may be a consequence of restricted rotation about the P—C (ipso-mesityl) bond. Additionally, there is considerable broadening of the resonance assigned to the ortho-methyl mesityl carbon ($\delta = 23.8$) in the $^{13}\mathrm{C}\{^{1}\mathrm{H}\}$ NMR spectrum. Another interesting feature in the $^{1}\mathrm{H}$ NMR spectrum of **4b** is

---

[2] Supplementary data for this article are available on the journal Web site (canjchem.nrc.ca) or may be purchased from the Depository of Unpublished Data, Document Delivery, CISTI, National Research Council Canada, Ottawa, ON K1A 0R6, Canada. DUD 5227. For more information on obtaining material, refer to cisti-icist.nrc-cnrc.gc.ca/irm/unpub_e.shtml. CCDC 655085 (**4a**), 655086 (**7a**), 655087 (**8a**), and 655088 (**9a**) contain the crystallographic data for this manuscript. These data can be obtained, free of charge, via www.ccdc.cam.ac.uk/conts/retrieving.html (or from the Cambridge Crystallographic Data Centre, 12 Union Road, Cambridge CB2 1EZ, UK; fax +44 1223 336033; or deposit@ccdc.cam.ac.uk).

[3] The ligand cone angle θ was estimated according to Tolman's method for an unsymmetrical phosphine ($\mathrm{PR_1R_2R_3}$) ligand. The cone angle is the apex angle of a cylindrical cone centrally positioned 2.28 Å away from the P. The edges of the cylindrical cone encompassed the van der Waals radii of the outermost atoms on each substituent on P. Using X-ray crystallographic data for **4a**, θ was estimated to be ~140°.

Scheme 2. Initiation of **1** with alkyllithium reagents and subsequent termination with electrophiles.

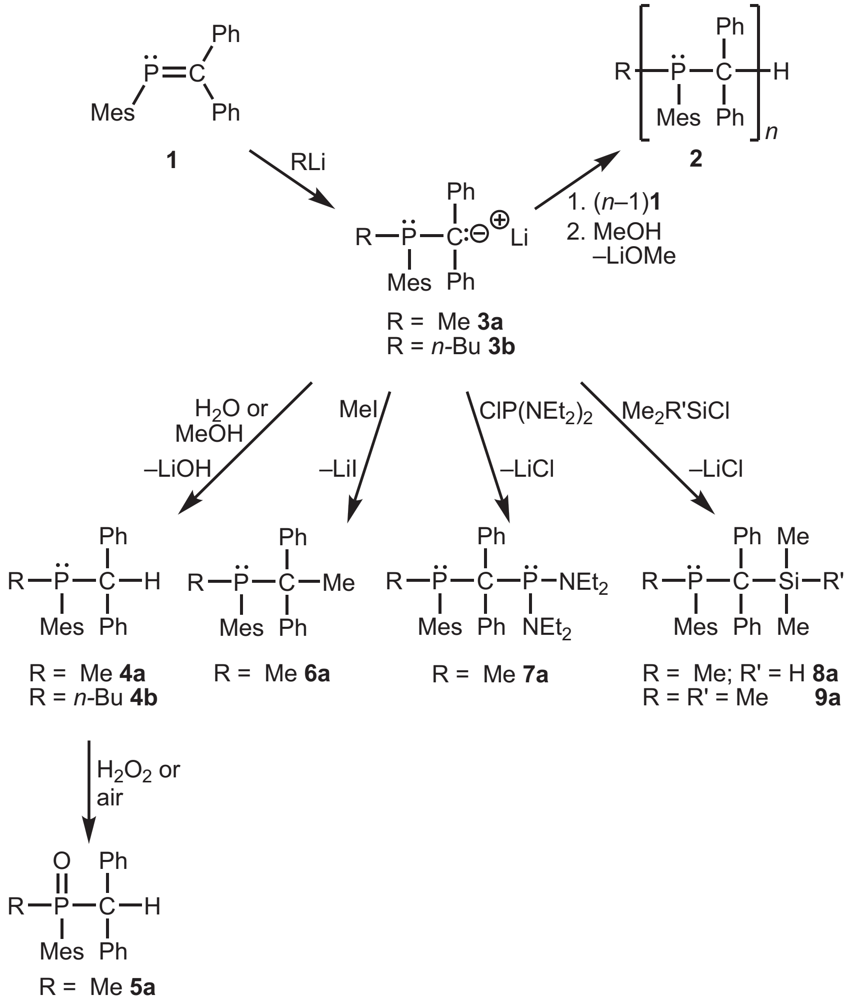

the diastereotopic protons adjacent to the stereogenic phosphorus atom. In particular, they give rise to two sets of multiplets (δ = 2.02 and 1.55). Assignments were made with the help of ^{1}H–^{1}H COSY, HMQC, and HMBC experiments.

To model the end-functionalization of polymer **2**, we investigated the termination of the methyl-initiated species **3a** with different electrophiles. These end-functionalized products are envisaged as model systems for the heretofore-unknown telechelic polymers.

To obtain Me-terminated **6a**, carbanion **3a** was quenched with neat methyl iodide, affording an orange solution ($\delta_{^{31}P}$ = –13.5). Model compound **6a** was characterized by ^{1}H, ^{13}C{^{1}H}, and ^{31}P NMR spectroscopy and low resolution EI-MS (M$^+$, *m*/*z* = 346). Although analytically pure material could not be isolated, analysis by NMR spectroscopy suggests 95% or higher purity. As with butyl-initiated **4b**, the signal assigned to the ortho-methyl mesityl protons in the ^{1}H NMR spectrum (δ = 1.87) is broad. Two doublets are observed in the alkyl region (1.70 ppm, $^2J_{PH}$ = 13 Hz; 1.39 ppm, $^3J_{PH}$ = 7 Hz). The resonance with the larger P–H coupling constant is assigned to the P-CH$_3$ group whilst the other signal is attributed to the quenching methyl group.

Phosphine end-functionalized **7a** was prepared by quenching **3a** with a solution of ClP(NEt$_2$)$_2$ (1.1 equiv.) in THF. The crude diphosphine was purified by washing the solid with cold hexanes (–78 °C). As expected, the ^{31}P{^{1}H} NMR spectrum of the product showed that the phosphorus atoms are inequivalent and are observed as two doublets (P2: δ = 105.3, P1: δ = –9.4; $^2J_{pp}$ = 205 Hz). The observed coupling constant is considerably larger than in a related asymmetric diphosphine [$Ph_2PCH_2P(NC_4H_4)_2$, $^2J_{PP}$ = 147 Hz] (27) and suggests some direct P–P interaction. In contrast to the broadened signals observed in **4b** and **6a**, the ortho-methyl mesityl groups in **7a** are inequivalent in both the ^{1}H and ^{13}C{^{1}H} NMR spectra. Presumably, this results from restricted rotation due to the increased steric bulk in **7a**.

X-ray-quality crystals of **7a** were grown from toluene. Crystallographic data are shown in Fig. 2, Table 1, and the Supplementary data.[2] Interestingly, the P(1)–C(11)–P(2) bond angle (99.17(9)°) is more acute than a typical sp^3-hybridized C atom. This small bond angle, combined with the short P···P distance [P(1)—P(2) = 2.966(1) Å, cf. Σ r_{vdw} = 3.7 Å], may account for the large coupling constant ($^2J_{PP}$) observed in solution. To confirm that the structure observed in solution is the same as that in the solid state, a solid-state ^{31}P NMR spectrum was recorded, which revealed a similarly large coupling constant ($^2J_{PP}$ = 255 Hz). Surprisingly, both nitrogen atoms are planar with the sum of the bond angles at nitrogen totaling 360°. Likely, the planarity is due to donation of nitrogen electron density into P(2), and this notion is

Table 1. X-ray crystallographic data of **4a**, **7a**, **8a**, and **9a**.

Crystal	**4a**	**7a**	**8a**	**9a**
Formula	$C_{23}H_{25}P$	$C_{31}H_{44}N_2P_2$	$C_{25}H_{31}PSi$	$C_{26}H_{33}PSi$
Formula weight	332.40	506.62	390.56	404.58
Crystal system	monoclinic	monoclinic	monoclinic	triclinic
Space group	$P2_1/c$	$P2_1/n$	$C2/c$	$P\bar{1}$
Color	colorless	colorless	colorless	colorless
a (Å)	18.867(2)	9.528(5)	20.677(5)	9.165(5)
b (Å)	6.1290(5)	15.614(5)	8.955(5)	10.757(5)
c (Å)	16.618(2)	18.935(5)	23.987(5)	12.689(5)
α (°)	90	90	90	79.511(5)
β (°)	92.401(3)	94.828(5)	101.555(5)	71.398(5)
γ (°)	90	90	90	75.169(5)
V (Å^3)	1919.9(3)	2807.0(19)	4351(3)	1143.3(9)
Z	4	4	8	2
T (K)	173(2)	173(2)	173(2)	173(2)
μ(Mo Kα) (cm^{-1})	1.44	1.77	1.89	1.82
Crystal size (mm)	0.2 × 0.2 × 0.1	1.4 × 0.6 × 0.4	1.4 × 1.2 × 1.0	1.0 × 1.0 × 0.5
$D_{\text{calcd.}}$ (g cm^{-3})	1.150	1.199	1.192	1.175
2θ(max) (°)	56.02	56.04	56.36	55.66
No. of reflections	26221	27995	54740	27579
No. of unique data	4580	6560	5281	5333
R_{int}	0.040	0.050	0.033	0.024
Reflections/parameters ratio	20.82	12.84	14.35	13.85
R_1, wR_2 [$I > 2\sigma(I)$]^a	0.0388, 0.0925	0.0418, 0.0944	0.0350, 0.0883	0.0306, 0.0820
R_1, wR_2 (all data)^a	0.0662, 0.1015	0.0787, 0.1149	0.0446, 0.0950	0.0354, 0.0862
GOF	1.053	1.017	1.029	1.054

$^a R_1 = \Sigma|(|F_o| - |F_c|)|/\Sigma|F_o|$. $wR_2 = [\Sigma(F_o^2 - F_c^2)^2/\Sigma w(F_o^2)^2]^{1/2}$.

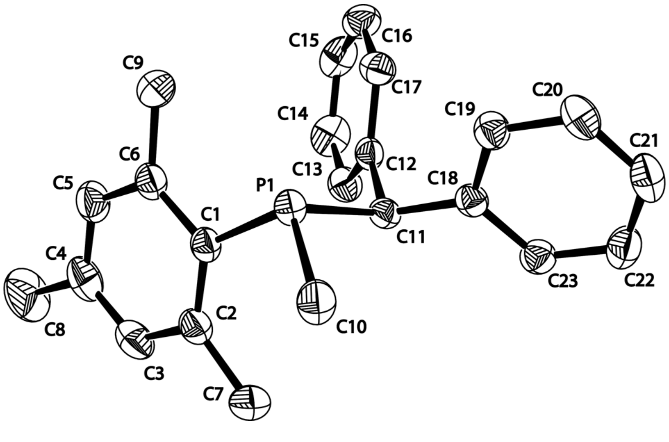

Fig. 1. Molecular structure of **4a** (50% probability ellipsoids). Hydrogen atoms are omitted for clarity. Selected bond lengths (Å): P(1)—C(1) = 1.852(1); P(1)—C(10) = 1.840(2); P(1)—C(11) = 1.882(1). Selected bond angles (°): C(10)–P(1)–C(1) = 107.34(7); C(10)–P(1)–C(11) = 100.51(7); C(1)–P(1)–C(11) = 100.18(6).

reinforced by the short P—N distances; P(2)—N(1) = 1.678(2) and P(2)—N(2) = 1.689(2) Å (28). In related bis(amino)phosphines, the P—N bonds are often shortened to 1.6–1.7 Å, which is accompanied by planarity at the nitrogen (29–32). Also, addition of the functional end-group lengthens the backbone P—C bonds to beyond typical single bonds [P(1)—C(11) = 1.942(2) and P(2)—C(11) = 1.951(2) Å] (28).

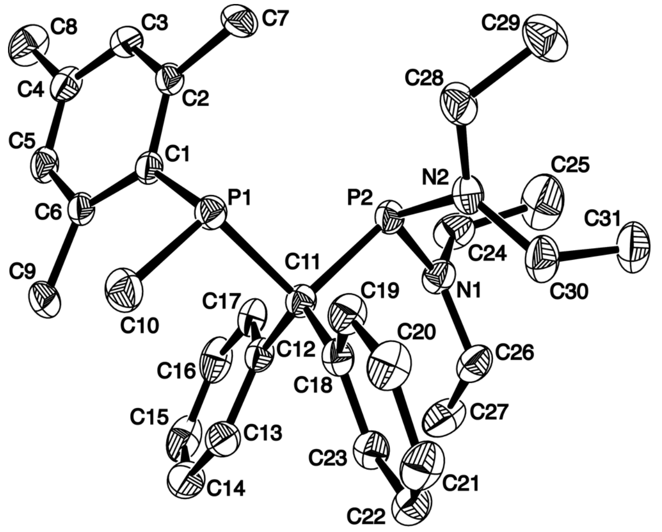

Fig. 2. Molecular structure of **7a** (50% probability ellipsoids). Hydrogen atoms are omitted for clarity. Selected bond lengths (Å): P(1)—C(1) = 1.851(2); P(1)—C(10) = 1.843(2); P(1)—C(11) = 1.942(2); P(2)—C(11) = 1.951(2); P(2)—N(1) = 1.678(2); P(2)—N(2) = 1.689(2); P(1)···P(2) = 2.966(1). Selected bond angles (°): C(1)–P(1)–C(10) = 105.1(1); C(1)–P(1)–C(11) = 110.05(9); C(10)–P(1)–C(11) = 101.5(1); P(1)–C(11)–P(2) = 99.17(9); C(11)–P(2)–N(1) = 103.87(8); C(11)–P(2)–N(2) = 105.97(9); N(1)–P(2)–N(2) = 107.80(9); Σ angles about N(1) atom = 359.7(3)°; Σ angles about N(2) atom = 359.4(3)°.

Addition of Me_2HSiCl or Me_3SiCl to carbanion **3a** produced silane end-functionalized **8a** and **9a**, respectively. These compounds formed quantitatively from **3a** according to the ^{31}P NMR spectra of the reaction mixtures (**8a**: δ = –23.9, **9a**: δ = –25.4); however, their high solubility resulted in low isolated yields of pure product after recrystallization (**8a**: 50%, **9a**: 14%). Analogous to that mentioned previously for **7a**, the ^1H NMR signals for the ortho-methyl protons of the mesityl group were inequivalent, and two broad signals were observed (**8a**: δ = 3.1 and 1.1, **9a**: δ = 2.8 and 0.9). Importantly, for **8a**, a singlet resonance is observed at 4.58 ppm, which is assigned to the Si–H proton. Although the methyl protons of the $SiMe_3$ moiety are equivalent in **9a**, the methyl protons of the $SiMe_2H$ moiety are inequivalent in **8a**. In particular, the $SiHMe_2$ group in **8a** shows two sets of doublets at 0.10 ppm ($^3J_{HH}$ = 3 Hz) and 0.05 ppm ($^3J_{HH}$ = 3 Hz). Both **8a** and **9a** were also characterized by low resolution EI-MS (M^+: *m/z* = 390 for **8a** and 404 for **9a**), elemental analysis (**8a** only), and X-ray crystallography.

Crystals of **8a** and **9a** were obtained from hexanes. The molecular structures and important lengths and angles are given in Figs. 3 and 4, and additional data is provided in Table 1 and the Supplementary data.[2] As with the other model compounds, **4a** and **7a**, the P—CPh_2H bond lengths [**8a**: P(1)—C(11) = 1.902(1), **9a**: P(1)—C(1) = 1.920(1) Å] are significantly longer than the two other P—C bonds [avg. for **8a** and **9a** = 1.835(5) Å]. Similar to that discussed previously, this elongation may be attributed to steric congestion. The small size of the $SiMe_2H$ moiety compared with the $SiMe_3$ moiety is reflected by the smaller P–C–Si bond angles in **8a** [**8a**: P(1)–C(11)–Si(1) = 106.57(6)°, **9a**: P(1)–C(1)–Si(1) = 111.52(6)°]. Remarkably, these angles are much larger than the the analogous angle in diphosphine **7a** [P(1)–C(11)–P(2) = 99.17(9)°] in which we speculate there is a weak P···P interaction.

Summary

In closing, the initiation and termination steps in the anionic polymerization of P=C bonds have been modeled. The initiation step was investigated through the stoichiometric reaction of $MesP=CPh_2$ (**1**) with RLi (R = Me or *n*-Bu). In all cases, the addition was highly regioselective with the formal attack of R^- at phosphorus to give the carbanion Li[Mes(R)P–CPh_2] (**3a**/**3b**). To simulate the termination step in the anionic polymerization of **1**, carbanions **3a** and **3b** were quenched in situ with electrophiles such as a proton (from H_2O or MeOH), a methyl cation (from MeI), a phosphenium moiety (from $ClP(NEt_2)_2$), or a silylium moiety (from Me_2HSiCl or Me_3SiCl). In this way, five new tertiary phosphines and one diphosphine were accessed and will function as models for poly(methylenephosphine)s. Four of these molecules were characterized crystallographically.

In future, we will extend this chemistry to the polymer **2** with the goal of preparing end-functional telechelic polymers that can be employed in the synthesis of novel block copolymers. In addition, these new compounds will be used to prepare molecular complexes that will serve as models for macromolecular coordination complexes of poly(methylenephosphine)s.

Fig. 3. Molecular structure of **8a** (50% probability ellipsoids). Hydrogen atoms are omitted for clarity except for H(1). Selected bond lengths (Å): P(1)—C(1) = 1.834(2); P(1)—C(10) = 1.824(2); P(1)—C(11) = 1.902(1); Si(1)—C(11) = 1.910(2); Si(1)—C(24) = 1.855(2); Si(1)—C(25) = 1.849(2); Si(1)—H(1) = 1.36(2). Selected bond angles (°): C(1)–P(1)–C(10) = 107.39(7); C(1)–P(1)–C(11) = 106.61(6); C(10)–P(1)–C(11) = 102.33(7); P(1)–C(11)–Si(1) = 106.57(6).

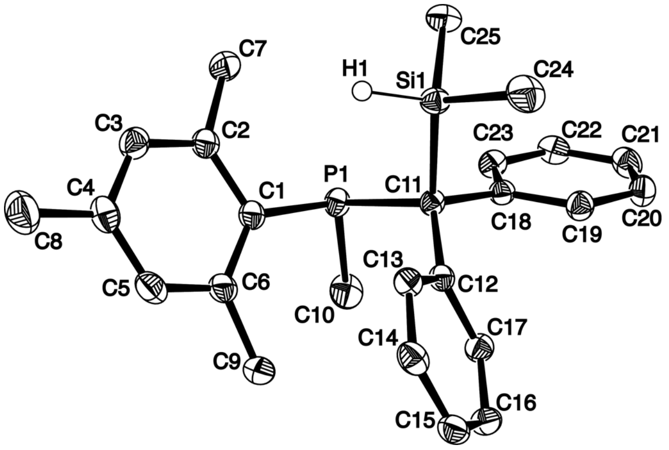

Fig. 4. Molecular structure of **9a** (50% probability ellipsoids). Hydrogen atoms are omitted for clarity. Selected bond lengths (Å): P(1)—C(1) = 1.920(1); P(1)—C(2) = 1.839(2); P(1)—C(3) = 1.844(1); C(1)—Si(1) = 1.944(1). Selected bond angles (°): C(1)–P(1)–C(2) = 101.38(6); C(2)–P(1)–C(3) 106.97(7); C(1)–P(1)–C(3) = 107.53(5); P(1)–C(1)–Si(1) = 111.52(6).

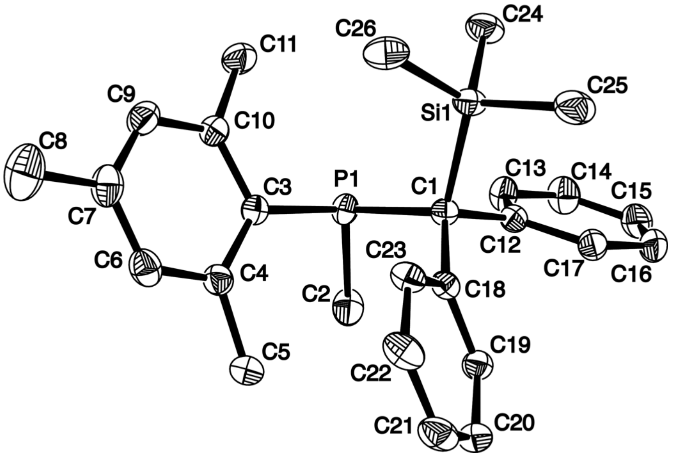

Experimental

Materials and general procedure

All manipulations of oxygen- and (or) moisture-sensitive compounds were performed under a nitrogen atmosphere using standard Schlenk and (or) glovebox techniques. Hexanes, diethyl ether, and dichloromethane were deoxygenated with nitrogen and dried by passing through a column containing activated alumina. THF was freshly distilled from sodium/benzophenone ketyl. Distilled water and methanol were degassed prior to use. $CDCl_3$ was distilled from P_2O_5 and degassed. CD_2Cl_2 and C_6D_6 were purchased from Cambridge Isotope Laboratories and were dried over molecular sieves (3 Å). PCl_3, $HNEt_2$, MeI, MeLi (1.6 mol/L in Et_2O), and *n*-BuLi (1.6 mol/L in hexanes) were purchased from Aldrich and used as received. Alkyllithium reagents were titrated prior to use. Me_2SiHCl and Me_3SiCl were distilled over CaH_2 and degassed prior to use. $MesP{=}CPh_2$, **1**, was prepared following literature procedures (21, 22). $ClP(NEt_2)_2$ was prepared from an adaptation of a literature method (33). A solution of $HNEt_2$ (190 mL, 1.84 mol) and CH_2Cl_2 (300 mL) was added slowly to a cooled (–78 °C) solution of PCl_3 (40 mL, 0.46 mol) in CH_2Cl_2 (250 mL). The reaction mixture was slowly warmed to room temperature and stirred for 1 h, and the solvent was removed in vacuo. The resulting solid was extracted with hexanes (3 × 150 mL) and filtered. Hexanes was removed in vacuo. The resulting oil was distilled under vacuum, yielding a colorless liquid (89 g, 92%). $^{31}P\{^1H\}$ NMR (C_6D_6, 121.5 MHz): δ = 154.8. ^1H NMR (C_6D_6, 300 MHz): δ = 2.9–3.1 (m, 8H, CH_2); 0.94 (t, 12H, $^3J_{HH}$ = 7 Hz, CH_3).

^{31}P, ^1H, and $^{13}C\{^1H\}$ NMR spectra were recorded on Bruker AV300 or AV400 spectrometers at room temperature. Solid-state NMR experiments were performed on a Bruker Avance DSX400 spectrometer operating at frequencies of 400.13 MHz and 161.98 MHz for ^1H and ^{31}P respectively, using a Bruker triple resonance 4mm MAS probe. Chemical shifts for ^{31}P NMR spectra are reported relative to H_3PO_4 as an external standard (85% in H_2O, δ = 0). Chemical shifts for $^{13}C\{^1H\}$ NMR spectra are reported relative to CD_2Cl_2 (δ = 54.0) or $CDCl_3$ (δ = 77.2). Chemical shifts for ^1H NMR spectra are reported relative to residual $CHDCl_2$ (δ = 5.32) or $CHCl_3$ (δ = 7.27) or C_6HD_5 (δ = 7.16). Mass spectra were recorded on a Kratos MS 50 instrument. Elemental analyses were performed by Mr. Minaz Lakha in the Departmental Microanalysis Facility.

Preparation of Mes(Me)P–CPh_2Li (3a)

Typical procedure

To a cooled (–78 °C) solution of phosphaalkene **1** (2.06 g, 6.5 mmol) in THF or Et_2O (~150 mL) was slowly added MeLi in Et_2O (5.2 mL, 1.5 mol/L, 7.8 mmol). Upon addition, there was an immediate color change from yellow to dark red. The cooled solution was stirred for 1 h and then warmed to room temperature where it was stirred for an additional 1 h. The concentration for use in subsequent steps was 0.043 mol/L (see preparation of **4a**). $^{31}P\{^1H\}$ NMR spectroscopy of an aliquot removed from the reaction mixture showed a single signal (δ = −42.0 in THF, −44.3 in Et_2O).

Preparation of Mes(*n*-Bu)P–CPh_2Li (3b)

To a stirred yellow solution of **1** (0.64 g, 2.0 mmol) in Et_2O (~30 mL) at –78 °C, a solution of *n*-BuLi in hexanes (3.0 mL, 1.4 mol/L, 4.2 mmol) was added rapidly. The mixture turned bright orange upon addition and was stirred at –78 °C for 30 min. Subsequently, the solution was warmed to room temperature where it was stirred for an additional 1 h. Over this time, the solution turned from bright orange to red. The reaction was monitored by $^{31}P\{^1H\}$ NMR spectroscopy, affording a single signal for **3b** (δ = –31.1). This solution was used in the preparation of **4b**.

Preparation of Mes(Me)P–CPh_2H (4a)

To a stirred red solution of **3a** in THF (150 mL, 0.043 mol/L, 6.4 mmol) was added degassed MeOH (0.4 mL). From the resultant colorless solution, THF was removed in vacuo, affording a white solid residue. The soluble fraction was extracted into hexanes (3 × 50 mL), and the resultant solution was evaporated to dryness, affording a yellow oil. The oil was dissolved in minimal hexanes at reflux (~5 mL). The solution was slowly cooled to room temperature to afford colorless crystals suitable for X-ray diffraction.

Yield: 0.50 g (24%). $^{31}P\{^1H\}$ NMR (CD_2Cl_2, 121.5 MHz): δ = –24.0 (s). ^1H NMR (CD_2Cl_2, 300 MHz): δ = 7.58 – 7.10 (m, 10H, Ph–*H*), 6.77 (s, 2H, *m*-Mes–*H*), 4.87 (d, $^2J_{HP}$ = 5 Hz, 1H, CPh_2H), 2.52 (s, 6H, *o*-Mes–CH_3), 2.21 (s, 3H, *p*-Mes–CH_3), 1.31 (d, $^2J_{HP}$ = 6 Hz, 3H, P–CH_3). $^{13}C\{^1H\}$ NMR (CD_2Cl_2, 75.5 MHz) (unassigned): δ = 146.0 (d, J_{CP} = 15 Hz), 144.3, 144.1, 144.0, 143.8 (4 × s or 2 × d), 140.4 (s), 131.4–127.4 (m), 52.8 (d, $^1J_{CP}$ = 16 Hz), 24.6, 24.4 (2 × s or 1 × d), 10.8 (d, $^1J_{CP}$ = 18 Hz, P–CH_3). MS (EI, 70 eV) *m/z* (%): 332 (28) [M^+], 167 (100) [$CHPh_2^+$], 165 (44) [$M^+ - CHPh_2$], 119 (12) [Mes^+].

Preparation of Mes(*n*-Bu)P–CPh_2H (4b)

To a stirred solution of carbanion **3b** in Et_2O (2.0 mmol) was added dropwise degassed H_2O until the reaction mixture turned pale yellow (several drops). The mixture was then dried with $MgSO_4$, filtered, and the soluble fraction was extracted with Et_2O (2 × 10 mL). The solvent was removed in vacuo at 60 °C to afford pure **4b** as a pale yellow oil.

Yield: 0.65 g (85 %). ^{31}P NMR (CD_2Cl_2, 121.5 MHz): δ = –12.4 (s). ^1H NMR (CD_2Cl_2, 400 MHz) (assignments made with the aid of a COSY experiment): δ = 7.57 (d, $^3J_{HH}$ = 8 Hz, 2H, Ph–*H*), 7.36 (m, 4H, Ph–*H*), 7.24 (m, 1H, Ph–*H*), 7.15 (m, 2H, Ph–*H*), 7.06 (m, 1H, Ph–*H*), 6.77 (br s, 2H, *m*-Mes–*H*), 4.91 (d, $^2J_{PH}$ = 5 Hz, 1H, CPh_2H), 2.56 (br s, 6H, *o*-Mes–CH_3), 2.20 (s, 3H, *p*-Mes–CH_3), 2.02 (m, 1H, P–CH*H*), 1.55 (m, 1H, P–C*H*H), 1.22 (m, 2H, $CH_2CH_2CH_3$), 1.08 (m, 2H, PCH_2CH_2), 0.74 (t, $^3J_{HH}$ = 7 Hz, 3H, CH_2CH_3). $^{13}C\{^1H\}$ NMR (CD_2Cl_2, 100.6 MHz) (assignments made with the aid of HMQC/HMBC experiments): δ = 143.6 (d, $^2J_{CP}$ = 12 Hz, *i*-Ph–*C*), 143.4 (d, $^2J_{CP}$ = 13 Hz, *i*-Ph–*C*), 139.5 (s, *p*-Mes–*C*), 130.2 (br, *m*-Mes–*C*), 129.7 (d, $^1J_{CP}$ = 26 Hz, *i*-Mes–*C*), 129.5 (d, $^3J_{CP}$ = 9 Hz, *o*-Ph–*C*), 129.1 (s, *o*-Mes–*C*), 128.9 (d, $^3J_{CP}$ = 9 Hz, *o*-Ph–*C*), 128.6 (s, *p*-Ph–*C*), 127.1 (d, $^4J_{CP}$ = 2 Hz, *m*-Ph–*C*), 126.5 (d, $^4J_{CP}$ = 2 Hz, *m*-Ph–*C*), 51.6 (d, $^1J_{CP}$ = 16 Hz, $CHPh_2$), 30.2 (d, $^2J_{CP}$ = 20 Hz, P–CH_2CH_2), 25.5 (d, $^1J_{CP}$ = 16 Hz, P–CH_2), 24.7 (d, $^3J_{CP}$ = 13 Hz, $CH_2CH_2CH_3$), 23.8 (v br, *o*-Mes–CH_3), 21.2 (s, *p*-Mes–CH_3), 14.1 (s, CH_2CH_3). MS (EI, 70 eV) *m/z* (%): 374 (29) [M^+], 167 (100) [CPh_2H^+], 151 (24) [$PMes^+$]. Found (calcd.) (%): C, 83.81 (83.39); H, 8.55 (8.34).

Synthesis of Mes(Me)P–CPh_2Me (6a)

MeI (1.6 mL, 26 mmol) was added dropwise to a solution of **3a** in Et_2O (160 mL, 0.16 mol/L, 26 mmol). The solution was stirred for 30 min over which time its color changed from red to orange. The solvent was removed in vacuo, the soluble fraction was extracted with hexanes, and evaporated to dryness. The product was purified by sublimation (140 °C, 0.1 mmHg).

Yield = 5.7 g (64 %). ^{31}P NMR ($CDCl_3$, 121.5 MHz): δ = –13.5 (s). ^{1}H NMR ($CDCl_3$, 300 MHz): δ = 7.47 (m, 2H, Ph–*H*), 7.21 (m, 6H, Ph–*H*), 7.01 (m, 2H, Ph–*H*), 6.74 (s, 2H, Mes–*H*), 2.23 (s, 3H, *p*-Mes–CH_3), 1.87 (br, 6H, *o*-Mes–CH_3), 1.70 (d, $^{2}J_{PH}$ = 13 Hz, 3H, P–CH_3), 1.39 (d, $^{3}J_{PH}$ = 7 Hz, 3H, CPh_2CH_3). ^{13}C{^{1}H} NMR ($CDCl_3$, 75.5 MHz,) (unassigned): δ = 148.3 (d, J_{CP} = 14 Hz), 146.3 (d, J_{CP} = 16 Hz), 144.7 (s), 138.8 (s), 129.9 (s), 128.7–127.4 (m), 125.8 (s), 125.4 (s), 49.1 (d, J_{CP} = 24 Hz), 28.8 (d, J_{CP} = 15 Hz), 23.5 (d, J_{CP} = 18 Hz), 20.8 (s), 9.0 (d, $^{1}J_{CP}$ = 21 Hz, P–*C*H_3). MS (EI, 70 eV) *m*/*z* (%): 346 (7) [M^+], 181 (100) [M^+ – P(Mes)(CH_3)], 165 (16) [M^+ – $CPh_2(CH_3)$], 119 (5) [Mes^+].

Preparation of Mes(Me)P–CPh_2–P$(NEt_2)_2$ (7a)

To a cooled (0 °C) solution of **3a** in THF (20 mL, 0.32 mol/L, 6.4 mmol) was slowly added a solution of ClP$(NEt_2)_2$ (1.50 g, 7.1 mmol) in THF (20 mL). An aliquot was removed from the yellow reaction mixture for ^{31}P NMR spectroscopic analysis. After evaporation of the volatiles in vacuo, the soluble fraction was extracted into toluene (30 mL). Removal of the toluene in vacuo afforded the crude product, which was washed with hexanes at –78 °C two times. Crystals suitable for X-ray diffraction were obtained from slow evaporation of a saturated toluene solution.

Yield: 1.73 g (54%). ^{31}P NMR ($CDCl_3$, 121.5 MHz): δ = 105.3 (d, $^{2}J_{PP}$ = 205 Hz, *P*N_2), –9.4 (d, $^{2}J_{PP}$ = 205 Hz, *P*Mes). ^{31}P MAS NMR (8.5 kHz, recycle delay of 20 s, 162.0 MHz): δ = 108.3 (d, $^{2}J_{PP}$ = 255 Hz, *P*N_2), –7.9 (d, $^{2}J_{PP}$ = 255 Hz, *P*Mes). ^{1}H NMR ($CDCl_3$, 400 MHz) δ = 7.79 (br, 2H, Ph–*H*), 7.43 (br, 2H, Ph–*H*), 7.28–7.14 (m, 6H, Ph–*H*), 6.90 (br, 1H, *m*-Mes–*H*), 6.55 (br, 1H, *m*-Mes–*H*), 3.01–2.52 (m, 11H, NCH_2 and *o*-Mes–CH_3), 2.25 (s, 3H, *p*-Mes–CH_3), 1.38 (d, $^{2}J_{PH}$ = 9 Hz, 3H, P–CH_3), 0.97 (m, 9H, NCH_2CH_3 and *o*-Mes–CH_3), 0.84 (t, 6H, $^{3}J_{HH}$ = 7 Hz, NCH_2CH_3). ^{13}C{^{1}H} NMR ($CDCl_3$, 100.6 MHz) (assignments made with the aid of HMQC/HMBC experiments): δ = 147.7 (s, *o*-Mes–*C*), 141.3 (br, Ar–*C*), 141.0 (t, J_{PC} = 5 Hz, Ar–*C*), 138.6 (s, *p*-Mes–*C*), 131.9–127.6 (m, Ar–*C*), 126.9 (s, Ar–*C*), 126.4 (s, Ar–*C*), 124.8 (d, J_{PC} = 4 Hz, Ar–*C*), 63.9 (dd, $^{1}J_{PC}$ = 46 and 34 Hz, P–*C*Ph_2–P), 44.5 (d, $^{2}J_{PC}$ = 21 Hz, N–*C*H_2), 44.0 (d, $^{2}J_{PC}$ = 20 Hz, N–*C*H_2), 26.2 (br s, *o*-Mes–*C*H_3), 21.6 (br s, *o*-Mes–*C*H_3), 21.0 (s, *p*-Mes–*C*H_3), 14.5 (d, $^{3}J_{PC}$ = 3 Hz, NCH_2CH_3), 14.0 (d, $^{3}J_{PC}$ = 5 Hz, NCH_2CH_3), 9.7 (t, $^{1}J_{PC}$ = 22 Hz, P–*C*H_3).

Preparation of Mes(Me)P–CPh_2–$SiMe_2H$ (8a)

To the red solution of **3a** (40 mL, 0.079 mol/L, 3.2 mmol) in THF (40 mL), neat Me_2HSiCl (0.5 mL, 4.6 mmol) was added. An immediate color change to yellow was observed. The solvent was removed in vacuo, and the residue was dissolved in hexanes (3 × 5 mL). Following solvent evaporation, the crude product was recrystallized from a minimal amount of hot hexanes in an inert atmosphere to afford large colorless crystals.

Yield: 0.62 g (50%). ^{31}P NMR (C_6D_6, 121.5 MHz): δ = –23.9 (s). ^{1}H NMR (C_6D_6, 300 MHz): δ = 7.70 (br s, 2H, Ph), 7.3–6.5 (m, 10H, Ph and *m*-Mes–*H*), 4.58 (br s, 1H, Si–*H*), 3.1 (br s, 3H, *o*-Mes–CH_3), 2.18 (s, 3H, *p*-Mes–CH_3), 1.45 (d, $^{2}J_{PH}$ = 8 Hz, 3H, P–CH_3), 1.1 (br s, 3H, *o*-Mes–CH_3), 0.10 (d, $^{3}J_{HH}$ = 3 Hz, 3H, Si–CH_3), 0.05 (d, $^{3}J_{HH}$ = 3 Hz, 3H, Si–CH_3). ^{13}C{^{1}H} NMR (CD_2Cl_2, 75.5 MHz) (assignments made with the aid of HMQC/HMBC experiments): δ = 147.6 (s, Mes–*C*), 147.3 (s, Mes–*C*), 142.5 (s, Mes–*C*), 142.1 (d, $^{1}J_{PC}$ = 7 Hz, *i*-Mes–*C*), 139.5 (s, Mes–*C*), 131–128 (m, Ph–*C*), 125.7 (s, Ph–*C*), 45.7 (d, $^{1}J_{PC}$ = 45 Hz, P*C*Ph_2), 21.2 (s, *p*-Mes–*C*H_3), 7.81 (d, $^{1}J_{PC}$ = 23 Hz, P*C*H_3), –3.96 (d, $^{3}J_{PC}$ = 5 Hz, Si*C*H_3), –5.66 (d, $^{3}J_{PC}$ = 6 Hz, Si*C*H_3). MS (EI, 70 eV) *m*/*z* (%): 390 (38) [M^+], 375 (17) [M^+ – CH_3], 332 (45) [M^+ – $SiMe_2$], 223 (69) [M^+ – PMesMe], 167 (100) [CPh_2^+]. Found (calcd.) (%): C, 77.20 (76.88); H, 7.64 (8.00).

Preparation of Mes(Me)P–CPh_2–$SiMe_3$ (9a)

To the red solution of **3a** in Et_2O (22 mL, 0.14 mol/L, 3.2 mmol), neat Me_3SiCl (0.4 mL, 3.2 mmol) was added. An immediate color change to yellow was observed accompanied by the formation of a white precipitate. The solution was filtered, the solvent was removed in vacuo, and the soluble fraction was extracted into Et_2O (3 × 15 mL). The Et_2O was removed in vacuo. The crude product was dissolved in a minimal amount of hexanes, and slow evaporation afforded colorless crystals suitable for X-ray crystallography.

Yield = 0.18 g (14%). ^{31}P NMR ($CDCl_3$, 121.5 MHz): δ = –25.4 (s). ^{1}H NMR ($CDCl_3$, 300 MHz): δ = 7.6 (br s, 2H, Ph), 7.3–7.1 (m, 8H, Ph), 6.8 (br s, 2H, *m*-Mes–*H*), 2.8 (br s, *o*-Mes–CH_3), 2.22 (s, 3H, *p*-Mes–CH_3), 1.33 (d, $^{2}J_{PH}$ = 8 Hz, 3H, P–CH_3), 0.9 (br s, 3H, *o*-Mes–CH_3), –0.02 (s, 9H, Si$(CH_3)_3$). MS (EI, 70 eV) *m*/*z* (%): 404 (100) [M^+], 389 (26) [M^+ – CH_3], 331 (44) [M^+ – $SiMe_3$], 167 (39) [M^+ – CPh_2SiMe_3], 73 (34) [M^+ – $MesMePCPh_2$].

X-ray crystallography

Crystal data and refinement parameters are listed in Table 1. Additional data are available in the Supplementary data.[2] All single crystals were immersed in oil and mounted on a glass fiber. Data for **4a** were collected on a Bruker X8 APEX diffractometer with graphite-monochromated Mo Kα radiation. Data for **7a**, **8a**, and **9a** were collected on a Bruker X8 APEX II diffractometer. Data were collected and integrated using the Bruker SAINT software package (34). All structures were solved by direct methods and subsequent Fourier difference techniques and were refined anisotropically for all non-hydrogen atoms. Hydrogen atoms were included in idealized positions and refined isotropically except in **4a** where they were not refined. All data sets were corrected for Lorentz and polarization effects. All calculations were performed using the SHELXTL crystallographic software package from Bruker-AXS (35).

Compounds **4a**, **8a**, and **9a** did not show any crystallographic complexity. Compound **7a** was a split crystal, and cell_now (within SAINT) was used to determine that the second domain was rotated from the first domain by 4.4°. Only the first domain was integrated because there was little or no overlap between the two lattices. One of the ethyl groups was disordered at C(28) and C(29). The disorder at carbon was modeled by including two additional carbon atoms [C(28b) and C(29b)] and refining their respective populations [occupancy: 0.78(2) and 0.22(2)].

Acknowledgement

This work was supported by the Natural Sciences and Engineering Research Council (NSERC) of Canada. The Canada Foundation for Innovation (CFI) and The British Columbia Knowledge Development Fund (BCKDF) are gratefully acknowledged for infrastructure support. The authors wish to thank to Dr. Brian O. Patrick for assistance with X-ray crystallography and Dr. Richard Darton and Professor Colin Fyfe for acquiring the solid-state NMR spectrum of **7a**.

References

1. K.B. Dillon, F. Mathey, and J.F. Nixon. Phosphorus: the carbon copy. Wiley, West Sussex, England. 1998.
2. F. Mathey. Angew. Chem., Int. Ed. **42**, 1578 (2003).
3. R. Appel. *In* Multiple bonds and low coordination in phosphorus chemistry. *Edited by* M. Regitz and O.J. Scherer. Thieme, Stuttgart. 1990. Chap. D4.
4. P. Le Floch. Coord. Chem. Rev. **250**, 627 (2006).
5. M. Freytag, S. Ito, and M. Yoshifuji. Chem. Asian J. **1**, 693 (2006).
6. B. Deschamps, X. Le Goff, L. Ricard, and P. Le Floch. Heteroat. Chem. **18**, 363 (2007).
7. L. Weber. Angew. Chem., Int. Ed. **41**, 563 (2002).
8. T. Baumgartner and R. Réau. Chem. Rev. **106**, 4681 (2006).
9. V.A. Wright, B.O. Patrick, C. Schneider, and D.P. Gates. J. Am. Chem. Soc. **128**, 8836 (2006).
10. V.A. Wright and D.P. Gates. Angew. Chem., Int. Ed. **41**, 2389 (2002).
11. K.J.T. Noonan and D.P. Gates. Angew. Chem., Int. Ed. **45**, 7271 (2006).
12. C.-W. Tsang, M. Yam, and D.P. Gates. J. Am. Chem. Soc. **125**, 1480 (2003).
13. C.-W. Tsang, B. Baharloo, D. Riendl, M. Yam, and D.P. Gates. Angew. Chem., Int. Ed. **43**, 5682 (2004).
14. B.H. Gillon and D.P. Gates. Chem. Commun. 1868 (2004).
15. T.A. van der Knaap and F. Bickelhaupt. Tetrahedron Lett. **23**, 2037 (1982).
16. B.-L. Li and R.H. Neilson. Inorg. Chem. **23**, 3665 (1984).
17. Z.-M. Xie, P. Wisian-Neilson, and R.H. Neilson. Organometallics, **4**, 339 (1985).
18. R. Appel, C. Casser, and F. Knoch. Chem. Ber. **119**, 2609 (1986).
19. For examples, see: (*a*) S. Ito, H. Miyake, M. Yoshifuji, T. Höltzl, and T. Veszprémi. Chem. Eur. J. **11**, 5960 (2005); (*b*) S. Ito, H. Miyake, H. Sugiyama, and M. Yoshifuji. Tetrahedron Lett. **45**, 7019 (2004); (*c*) A. Moores, L. Ricard, and P. Le Floch. Angew. Chem., Int. Ed. **42**, 4940 (2003); (*d*) G. Märkl and A. Merz. Tetrahedron Lett. **32**, 3611 (1968); (*e*) G. Märkl, F. Lieb, and A. Merz. Angew. Chem., Int. Ed. **6**, 87 (1967).
20. For examples, see: (*a*) S. Ito, M. Freytag, and M. Yoshifuji. Dalton Trans. 710 (2006); (*b*) S. Ito, K. Toyota, and M. Yoshifuji. Chem. Commun. 1637 (1997); (*c*) M. Yoshifuji, H. Kawanami, Y. Kawai, K. Toyota, M. Yasunami, T. Niitsu, and N. Inamoto. Chem. Lett. 1053 (1992); (*d*) S. J. Goede, and F. Bickelhaupt. Chem. Ber. **124**, 2677 (1991).
21. G. Becker, W. Uhl, and H.-J. Wessely. Z. Anorg. Allg. Chem. **479**, 41, (1981).
22. M. Yam, J.H. Chong, C.W. Tsang, B.O. Patrick, A.E. Lam, and D.P. Gates. Inorg. Chem. **45**, 5225 (2006).
23. For details of the Tolman method, see: C.A. Tolman. Chem. Rev. **77**, 313 (1977).
24. CRC handbook of chemistry and physics. 84th ed. CRC Press, Boca Raton, Florida. 2003.
25. P. Maire, S. Deblon, F. Breher, J. Geier, C. Böhler, H. Rüegger, H. Schönberg, and H. Grützmacher. Chem. Eur. J. **10**, 4198 (2004).
26. B. Manz, and G. Maas. J. Chem. Soc., Chem. Commun. 25 (1995).
27. A.D. Burrows, M.F. Mahon, S.P. Nolan, and M. Varrone. Inorg. Chem. **42**, 7227 (2003).
28. L. Pauling. The nature of the chemical bond and the structure of molecules and crystals: an introduction to modern structural chemistry. 3rd ed. Cornell University Press, New York. (1960).
29. P.W. Dyer, J. Fawcett, M.J. Hanton, R.D.W. Kemmitt, R. Padda, and N. Singh. Dalton Trans. 104 (2003).
30. F. Dahan, P.W. Dyer, M.J. Hanton, M. Jones, D.M.P. Mingos, A.J.P. White, D.J. Williams, and A.M. Williamson. Eur. J. Inorg. Chem. 732 (2002).
31. I. Shevchenko, V. Andrushko, E. Lork, and G.V. Röschenthaler. Eur. J. Inorg. Chem. 2985 (2002).
32. S.A. Reiter, S.D. Nogai, and H. Schmidbaur. Dalton Trans. 247 (2005).
33. P.G. Chantrell, C.A. Pearce, C.R. Torer, and R.J. Twaits. J. Appl. Chem. **14**, 563 (1964).
34. SAINT V [computer program]. 7.03A ed. Bruker AXS Inc., Madison, Wisconsin. 1997–2003.
35. SHELXTL V [computer program]. 5.1 ed. Bruker AXS Inc., Madison, Wisconsin. 1997.